Decomposition of the relativistic hyperfine interaction operator: Application to the ferromagnetic alloy systems fcc Fe_xNi_{1-x}, fcc Fe_xPd_{1-x}, and fcc Co_xPt_{1-x}

M. Battocletti and H. Ebert
Department Chemie-Physikalische Chemie, Universität München, Butenandtstrasse 5-13, D-81377 München, Germany
(Received 30 January 2001; published 8 August 2001)

A scheme developed by Pyper to decompose within relativistic Hartree-Fock theory the hyperfine interaction operator into the conventional Fermi contact, spin dipolar and orbital contributions is modified to split the hyperfine field of magnetic solids calculated in a fully relativistic way on the basis of spin-density-functional theory in an analogous way. The resulting expressions are used to examine the hyperfine fields for the disordered alloy systems fcc Fe_xNi_{1-x}, fcc Fe_xPd_{1-x}, and fcc Co_xPt_{1-x} making use of the spin-polarized relativistic Korringa-Kohn-Rostoker coherent-potential approximation method of band-structure calculation. In particular the contribution of non-*s* electrons to the hyperfine fields are discussed in detail. Special emphasize is laid on their relationship to the corresponding contributions to the spin and spin-orbit-induced orbital magnetic moments.

DOI: 10.1103/PhysRevB.64.094417 PACS number(s): 75.20.En, 71.15.Mb, 71.20.Be, 31.30.Gs

I. INTRODUCTION

A sound theoretical description of the magnetic hyperfine interaction was first given by Fermi[1] in 1930. Starting from the Dirac equation he found for the nonrelativistic limit three distinct contributions to the magnetic hyperfine interaction operator H_{hf} (a straightforward nonrelativistic derivation for these contributions can be found, for example, in Ref. 2). The first one is the Fermi-contact contribution H_F that stems from the spin magnetic moment of the electrons. Because it is proportional to the delta function $\delta(\vec{r})$, with the nuclear position at $\vec{r}=0$, only *s* electrons contribute to the hyperfine field of spontaneously magnetized solids via H_F. The other two contributions to H_{hf} are the spin dipolar and orbital contributions, H_{dip} and H_{orb}, respectively. In contrast to H_F, only electronic states with an orbital angular momentum $l \neq 0$ would contribute to hyperfine fields via these terms. However, the hyperfine fields corresponding to H_{orb} vanish within a nonrelativistic or scalar relativistic calculation because the electronic orbital angular momentum is quenched if the spin-orbit-coupling is neglected. (Here one should note that there are nevertheless contributions, for example, to the spin-lattice relaxation rate due to H_{orb}.) For lattice sites with cubic symmetry there are no contributions to the hyperfine fields due to H_{dip}. For a lower symmetry this term gives rise to an anisotropy that is normally relatively small.[3] As a consequence, in calculating the hyperfine fields of magnetic solids normally only the Fermi contact term H_F is considered.

Because of the spatial dependence of the hyperfine interaction operator and the conventional relativistic corrections (spin-orbit-coupling, mass velocity, and Darwin terms) to the Schrödinger equation it is quite obvious that the influence of relativistic effects shows up already for relatively light nuclei. Unfortunately, many authors tried to take this situation into account by including the so-called scalar-relativistic mass velocity and Darwin corrections only in the calculation of the electronic band structure while the hyperfine field interaction operator was left unchanged. On the other hand, starting from an expansion of the relativistic electronic wave function in powers of (Z/c),[4,5] Breit derived relativistic corrections to the Fermi-contact term.[6] This line was also followed by many other authors as for example by Pyykkö and his coworkers.[7] These authors also pointed out that the use of a scalar-relativistic Hamiltonian for the band-structure calculation is not compatible with the nonrelativistic expression for the Fermi contact hyperfine Hamiltonian H_F.[8] In particular it was found that this inconsistent approach leads to hyperfine fields that are much too large.[8,9] Among others this was demonstrated by the work of Blügel *et al.*[10] Starting from a decompostion of the relativistic hyperfine Hamiltonian these authors in addition derived an expression for H_F that is consistent with a scalar-relativistic band-structure calculation and that is generally accepted now.

Apart from the approach to account for relativistic influences on the hyperfine interaction by including corresponding corrections, several investigations can be found in the literature that are based on the Dirac equation and the proper relativistic form of the hyperfine interaction operator H_{hf} (Ref. 11) (see below). For solids the first steps in this direction have been made by Tterlikkis *et al.*[12] Calculating the hyperfine field of the elemental ferromagnets Fe, Co, and Ni in a fully relativistic way, Ebert *et al.* could unambiguously determine the relativistic enhancement of these fields compared to a nonrelativistic calculation.[13] In addition, it could be demonstrated that there are quite appreciable contributions due to non-*s* electrons that are connected with the presence of the spin-orbit coupling. By corresponding calculations for disordered transition metal alloys, where one has the concentration as an independent parameter to vary, it could be shown that these non-*s* contributions to the hyperfine field go nicely parallel with the spin-orbit-induced orbital magnetic moments.[14] For that reason, these contributions to the hyperfine field were intuitively called orbital. This was supported by a further analysis of the data based on an expression due to Abragam and Pryce[15] that connects orbital contributions to the magnetic moment and the hyperfine field. To allow for a more detailed and sound analysis of

hyperfine fields based on the relativistic hyperfine interaction operator H_{hf}, Ebert suggested to perform a Gordon decomposition of the electronic current density and derived this way a consistent relativistic counterpart to the nonrelativistic spin dipolar hyperfine interaction operator H_{dip}.[16] This approach was also used by Pyper who performed a complete decomposition of H_{hf} within the framework of Hartree-Fock theory.[17] As it will be shown below, this approach can be transferred with minor modifications to the treatment of magnetic solids done on the basis of spin-density-functional theory.

In the following section the relativistic calculation of hyperfine fields for magnetic solids will be reviewed in short. This is followed by a derivation of the relativistic expression for the Fermi contact, spin dipolar, and orbital hyperfine fields. Results obtained for the disordered alloy systems fcc Fe_xNi_{1-x}, fcc Fe_xPd_{1-x}, and fcc Co_xPt_{1-x} will be presented in Sec. III and discussed in some detail. A short summary and conclusions will be given at the end.

II. THEORETICAL FRAMEWORK

A. Electronic structure calculations

Within the present work we used the relativistic version of spin-density-functional theory (SDFT) (Refs. 18,19) to calculate the electronic structure of the investigated system in a self-consistent way. This implies in particular that the corresponding Dirac Hamiltonian H_D is given by

$$H_D = c\vec{\alpha}\cdot\vec{p} + \beta mc^2 + V(\vec{r}) + \beta\vec{\sigma}\cdot\vec{B}_{eff}(\vec{r}). \tag{1}$$

Here $\vec{\alpha}$ is the vector of 4×4 standard Dirac matrices[20] and $\vec{p}$ is the momentum operator. The potential $V(\vec{r})$ is the spin-independent part of the effective single-particle potential that consists in turn of its Coulomb and exchange correlation part. The spin-dependent part of the potential is represented by the effective magnetic field

$$\vec{B}_{eff}(\vec{r}) = \vec{B}_{ext}(\vec{r}) + \frac{\delta E_{xc}[n,\vec{m}]}{\delta\vec{m}(\vec{r})}. \tag{2}$$

In general an external field $\vec{B}_{ext}(\vec{r})$ may contribute to $\vec{B}_{eff}(\vec{r})$. Because we are interested in the following in spontaneously magnetized solids, this term can be ignored. The second contribution to $\vec{B}_{eff}(\vec{r})$ represents the spin polarization of the system and is expressed by the variation of the exchange-correlation energy E_{xc} with respect to the spin magnetization $\vec{m}(\vec{r})$. To emphasize the origin of $\vec{B}_{eff}(\vec{r})$ and to distinguish it from the hyperfine field B_{hf} to be introduced below, it will be denoted $\vec{B}_{xc}(\vec{r})$ in the following.

For transition metal systems calculations based on the SDFT give in general very good results for spin-magnetic moments. For the spin-orbit-induced orbital moments, however, the results are often found to be too small compared with experiment.[13] However, this shortcoming of plain SDFT does not affect the relationship between the orbital contribution to the magnetic moment and the hyperfine fields, that is one of the main issues of this study.

To deal with the Dirac equation based on the Hamiltonian given in Eq. (1), it is convenient to split the electronic system into a subsystem consisting of the tightly bound core electrons and one due to the valence-band electrons. Due to the spin-dependent term $\vec{B}_{xc}(\vec{r})$, the corresponding wave functions have in general no unique spin-angular character but are a superposition of various contributions. For the core wave functions $\Phi_{n\Lambda}$ one has for example[21]

$$\Phi_{n\Lambda}(\vec{r},E) = \sum_{\Lambda'} \Phi_{n\Lambda'\Lambda}(\vec{r},E), \tag{3}$$

where n is the principal quantum number and $\Lambda=(\kappa,\mu)$ combines the spin-orbit and magnetic quantum numbers. In Eq. (3) Λ indicates the spin-angular character of the dominating contribution to $\Phi_{n\Lambda}$, while Λ' gives the spin-angular character of the various contributions that have the conventional form:[20]

$$\Phi_{\Lambda'\Lambda}(\vec{r},E) = \begin{pmatrix} g_{\Lambda'\Lambda}(r,E)\chi_{\Lambda'}(\hat{r}) \\ if_{\Lambda'\Lambda}(r,E)\chi_{-\Lambda'}(\hat{r}) \end{pmatrix} \tag{4}$$

with $-\Lambda=(-\kappa,\mu)$. Here the large and small components are composed of the radial wave functions $g_{\Lambda'\Lambda}(r,E)$ and $f_{\Lambda'\Lambda}(r,E)$ and the spin-angular functions:[20]

$$\chi_\Lambda(\hat{r}) = \sum_{m_s=\pm1/2} C\left(l\,\frac{1}{2}\,j;\mu-m_s,m_s\right) Y_l^{\mu-m_s}(\hat{r})\chi_{m_s}, \tag{5}$$

with the Clebsch-Gordon coefficients $C(l\,\frac{1}{2}\,j;m_l,m_s)$.

Within the present work, the valence-band electrons are represented by the corresponding Green's function $G(\vec{r},\vec{r}\,',E)$, that is determined by the use of multiple scattering theory:[22,23]

$$\begin{aligned} G(\vec{r},\vec{r}\,',E) = {} & \sum_{\Lambda\Lambda'} Z_\Lambda^n(\vec{r},E)\,\tau_{\Lambda\Lambda'}^{nn'}(E)\,Z_{\Lambda'}^{n'\times}(\vec{r}\,',E) \\ & - \sum_\Lambda \left[Z_\Lambda^n(\vec{r},E) J_\Lambda^{n\times}(\vec{r}\,',E)\Theta(r'-r) \right. \\ & \left. + J_\Lambda^n(\vec{r},E) Z_\Lambda^{n\times}(\vec{r}\,',E)\Theta(r-r') \right]\delta_{nn'}, \end{aligned} \tag{6}$$

where the wave functions Z_Λ^n and J_Λ^n are the properly normalized regular and irregular solutions to the Dirac equation for a single atomic potential well at site n. As for the core wave functions $\Phi_{n\Lambda}$ they have in general no unique spin-angular character, i.e., they are given by expressions similar to Eqs. (3) and (4). The scattering path operator $\tau_{\Lambda\Lambda'}^{nn'}(E)$ accounts for all multiple scattering processes in the extended solid. Crudely spoken the imaginary part of the site-diagonal scattering path operator $\mathrm{Im}\,\tau_{\Lambda\Lambda'}^{nn}(E)$ can be seen as a measure for the Λ-like local density of states.

Representing the electronic structure in terms of the corresponding Green's function $G(\vec{r},\vec{r}\,',E)$ instead of using Bloch wave functions $\Psi_{n\vec{k}}(\vec{r},E_{n\vec{k}})$ and the associated eigenvalues $E_{n\vec{k}}$, has the great advantage that it is straightforward to deal with disordered alloys. This feature is exploited here

by making use of multiple-scattering theory in combination with the coherent-potential-approximation (CPA) alloy theory.[22]

B. Relativistic calculations of the hyperfine fields of magnetic solids

The relativistic form for the hyperfine interaction operator that describes the coupling of the electronic current density $\vec{j}=ec\vec{\alpha}$ to the vector potential $\vec{A}_n$ created by the nuclear magnetic dipole $\vec{\mu}_n$ was given by Breit:[11]

$$H_{hf}=e\vec{\alpha}\cdot\vec{A}_n(\vec{r}) \tag{7}$$

$$=e\vec{\alpha}\cdot(\vec{\mu}_n\times\vec{r})A_n(r), \tag{8}$$

where $A_n(r)$ represents the radial dependence of the nuclear vector potential. For a point nucleus $A_n(r)$ is simply given by r^{-3}.

According to the decomposition of the electronic system, the contributions of the tightly bound core electrons and of the valence band electrons to the hyperfine interaction energy E_{hf} are calculated separately. The contribution E_{hf}^{core} to E_{hf} stemming from the core electrons is obtained straightforwardly from the expression:[21]

$$E_{hf}^{core}=\sum_{n\Lambda}\langle\Phi_{n\Lambda}|H_{hf}|\Phi_{n\Lambda}\rangle. \tag{9}$$

In terms of the electronic Green's function the contribution of the valence-band electrons to E_{hf} is given by

$$E_{hf}^{val}=-\frac{1}{\pi}\mathrm{Tr}\ \mathrm{Im}\int^{E_F}dE\int d^3r H_{hf}G(\vec{r},\vec{r},E), \tag{10}$$

where the energy integration extends over the range of the occupied part of the valence band up to the Fermi energy E_F.

In dealing with the expectation values in Eqs. (9) and (10) or corresponding expressions (see below), the nuclear part of the combined nuclear and electronic wave function is not given explicitely here. In addition, for the sake of simplicity, a nucleus with spin quantum number $I=1$ is assumed. This simplifies the notation, but has no influence on the result for the hyperfine field B_{hf}, that is usually introduced to discuss the magnetic hyperfine interaction in spontaneously magnetized solids. The hyperfine field B_{hf} represents the nuclear Zeeman splitting and can be seen as an isotope-independent interaction parameter that is related to the hyperfine interaction energy E_{hf} by

$$B_{hf}=E_{hf}/\mu_n. \tag{11}$$

As for E_{hf}, the hyperfine field B_{hf} is split into its core and valence-band contributions B_{hf}^{core} and B_{hf}^{val}, respectively.

With the hyperfine interaction operator H_{hf} given in Eq. (10) replaced by the operator $\mu_B\beta l_z$ one gets the spin-orbit-induced orbital magnetic moment μ_{orb}.[13] Due to the angular momentum expansion of the Green's function implied by Eq. (6) one is immediately led to a corresponding decomposition of E_{hf} or B_{hf}, respectively, and μ_{orb}. As emphasized above, the contributions to the hyperfine field B_{hf} due to non-*s* electrons will vanish in the nonrelativistic limit and cubic symmetry. The inclusion of spin-orbit coupling, however, leads to nonzero contributions even for cubic symmetry (in fact the presence of a finite magnetization breaks the cubic symmetry even for a crystallographic cubic lattice site).[24] One therefore has to find out whether these hyperfine field contributions of non-*s* electrons are primarily due to their spin or orbital motion. A first answer to this question can be obtained by making use of an expression suggested in a somewhat different context by Abragam and Pryce.[15] For the present situation one may expect for a given l value that the orbital contributions $B_{orb,l}^{val}$ of the valence electrons to B_{hf} are connected to the corresponding contributions to μ_{orb} by

$$B_{orb,l}^{val(AP)}\approx 2\mu_B\langle r^{-3}\rangle_l\mu_{orb,l}. \tag{12}$$

For the applications to be presented below the angular momentum expansion has been restricted to $l_{max}=2$. This implies that Eq. (12) will be applied individually for *p* and *d* states.

C. Decomposition of the relativistic hyperfine operator

The expression given in Eq. (12) allows one only to estimate the orbital part of the non-*s*-hyperfine fields. A rigorous decomposition of the hyperfine field, on the other hand, can be obtained by a corresponding decomposition of the relativistic hyperfine Hamiltonian H_{hf}. This has been achieved by Blügel *et al.* using the elimination technique.[10] Although this approach has been worked out so far only for the case of a spin-independent potential, it nevertheless supplied a firm and consistent theoretical basis to deal with the Fermi-contact interaction on the basis of a scalar-relativistic band-structure calculation. As an alternative to the approach of Blügel *et al.*, a decomposition of the hyperfine field can also be achieved by a Gordon decomposition of the electronic current density in Eq. (7). Here we adapted the derivation given by Pyper, who considered all parts of H_{hf} or $\vec{j}$, respectively, within the framework of Hartree-Fock theory.

To account for the most general situation we start from the Dirac and its adjoint equation, that determine the so-called left- and right-hand solutions, Φ_Λ^L and Φ_Λ^R, respectively:[25,26]

$$H_D|\Phi_\Lambda^R\rangle=E_\Lambda|\Phi_\Lambda^R\rangle, \tag{13}$$

$$\langle\Phi_\Lambda^L|H_D^\dagger=E_\Lambda\langle\Phi_\Lambda^L|. \tag{14}$$

Using the Dirac Hamiltonian given in Eq. (1) together with atomic Rydberg units, one gets

$$|\Phi_\Lambda^R\rangle=\frac{2}{c^2}\beta(E_\Lambda-V-\beta\vec{\sigma}\cdot\vec{B}_{xc}-c\vec{\alpha}\cdot\vec{p})|\Phi_\Lambda^R\rangle, \tag{15}$$

$$\langle\Phi_\Lambda^L|=\langle\Phi_\Lambda^L|(E_\Lambda-V-\beta\vec{\sigma}\cdot\vec{B}_{xc}-c\vec{\alpha}\cdot\overleftarrow{p})\beta\frac{2}{c^2}. \tag{16}$$

A Gordon decomposition of the electronic current density can be achieved now by starting from the expression

$$E_{hf}=\frac{1}{2}(\langle\Phi^L_\Lambda|H_{hf}|\Phi^R_{\Lambda'}\rangle+\langle\Phi^L_\Lambda|H_{hf}|\Phi^R_{\Lambda'}\rangle). \quad (17)$$

Inserting Eqs. (15) and (16) into the second and first term, respectively, of Eq. (17), one is led to three distinct contributions to E_{hf}:

$$E^E_{hf}=\frac{\mu_B}{c}\langle\Phi^L_\Lambda|E_\Lambda\beta\vec{\alpha}\cdot\vec{A}_n+\vec{\alpha}\cdot\vec{A}_n\beta E_{\Lambda'}|\Phi^R_{\Lambda'}\rangle \quad (18)$$

$$E^{SO}_{hf}=\mu_B\langle\Phi^L_\Lambda|-\vec{\alpha}\cdot\vec{p}\beta\vec{\alpha}\cdot\vec{A}_n-\vec{\alpha}\cdot\vec{A}_n\beta\vec{\alpha}\cdot\vec{p}|\Phi^R_{\Lambda'}\rangle \quad (19)$$

$$E^V_{hf}=\frac{\mu_B}{c}\langle\Phi^L_\Lambda|-(V+\beta\vec{\sigma}\cdot\vec{B}_{xc})\beta\vec{\alpha}\cdot\vec{A}_n - \vec{\alpha}\cdot\vec{A}_n\beta(V+\beta\vec{\sigma}\cdot\vec{B}_{xc})|\Phi^R_{\Lambda'}\rangle. \quad (20)$$

Using the energy-dependent term E^E_{hf} in Eq. (18) in connection with Eq. (9) or Eq. (10), respectively, one has $E_\Lambda=E_{\Lambda'}$. As a consequence, the contribution E^E_{hf} vanishes exactly because of the relation $\beta\alpha_i=-\alpha_i\beta$. Concerning the potential-dependent term E^V_{hf} in Eq. (20) one can see that this term vanishes also for the same reason if $\vec{B}_{xc}=0$. For a finite field $\vec{B}_{xc}\neq 0$ one has instead,

$$E^V_{hf}=-\frac{\mu_B}{c}\langle\Phi^L_\Lambda|(\vec{\sigma}\cdot\vec{B}_{xc})(\vec{\alpha}\cdot\vec{A}_n)+(\vec{\alpha}\cdot\vec{A}_n)(\vec{\sigma}\cdot\vec{B}_{xc})|\Phi^R_{\Lambda'}\rangle. \quad (21)$$

Replacing $\vec{\alpha}$ by $\gamma_5\vec{\sigma}$ where

$$\gamma_5=\begin{pmatrix}0 & I_2\\ I_2 & 0\end{pmatrix}$$

(I_2 is the 2×2 unit matrix) is one of the Dirac matrices[20] and making use of the relation

$$(\vec{\sigma}\cdot\vec{A}_n)(\vec{\sigma}\cdot\vec{B}_{xc})=\vec{A}_n\cdot\vec{B}_{xc}+i\vec{\sigma}(\vec{A}_n\times\vec{B}_{xc}), \quad (22)$$

one ends up with

$$E^V_{hf}=-2\frac{\mu_B}{c}\langle\Phi^L_\Lambda|\gamma_5\vec{A}_n\cdot\vec{B}_{xc}|\Phi^R_{\Lambda'}\rangle. \quad (23)$$

In general one assumes for the Dirac Hamiltonian in Eq. (1) that the magnetization within an atomic cell points along a unique direction $\hat{e}_z$ that is not necessarily identical with the crystallographic z axis. In that case the spin-dependent term of the potential is simply given by $\beta\sigma_z B_{xc}(\vec{r})$. The nuclear spin, on the other hand, will be aligned along the direction of the magnetization, i.e., the local z axis. As a consequence, the resulting vector potential $\vec{A}_n(\vec{r})$ will always be perpendicular to $\vec{B}_{xc}(\vec{r})=B_{xc}(\vec{r})\hat{e}_z$. This means that the contribution E^V_{hf}, as given by Eq. (23), will also vanish. For the more general situation, where one allows the field $\vec{B}_{xc}(\vec{r})$ to vary its orientation within an atomic cell,[27] there might be a contribution due to E^V_{hf}. For a highly symmetric field $\vec{B}_{xc}(\vec{r})$, however, it will still vanish because of cancellations in the integral in Eq. (23). Finally, the factor $1/c$ will ensure that a finite result for E^V_{hf} will be small compared to the term E^{SO}_{hf} to be discussed in detail below.

The above discussion of E^V_{hf} was based on the SDFT Hamiltonian given in Eq. (1). However, the same line of arguments apply if a more complex Hamiltonian is used, that is derived for example within the framework of current-density-functional theory (CDFT) (Ref. 28) or that includes Brooks' orbital polarization (OP) term.[29,30]

As discussed in detail by Pyper[17] the decomposition given by Eqs. (18)–(20) is only useful if the momentum operator $\vec{p}$ can be treated as an unitary operator, because otherwise one is led to surface integrals when dealing with Eq. (19). This requirement is automatically fulfilled if one accounts for the finite size of a nucleus. Assuming in particular a nuclear model, in which the entire nuclear magnetization resides on the surface of a sphere of finite radius r_n, one has for the radial distribution of the vector potential:[17]

$$A_n(r)=\begin{cases}\dfrac{1}{r_n^3} & \text{for} \quad r<r_n\\[2ex] \dfrac{1}{r^3} & \text{for} \quad r\geqslant r_n\,.\end{cases} \quad (24)$$

The term E^{SO}_{hf} in Eq. (19), that depends on the spin and orbital degree of freedom of the electron, can now be further transformed:

$$E^{SO}_{hf}=-i\mu_B\langle\Phi^L_\Lambda|[(\vec{\sigma}\cdot\vec{A}_n)(\vec{\sigma}\cdot\vec{\nabla})-(\vec{\sigma}\cdot\vec{\nabla})(\vec{\sigma}\cdot\vec{A}_n)]|\Phi^R_{\Lambda'}\rangle. \quad (25)$$

The term between the bra and ket can be identified with the corresponding hyperfine operator H^{SO}_{hf}:

$$H^{SO}_{hf}=-i\mu_B\beta\sum_{j\neq k}\sigma_j\sigma_k(\nabla_j A_{nk}+A_{nj}\nabla_k) - i\mu_B\beta\sum_j\sigma_j^2(\nabla_j A_{nj}+A_{nj}\nabla_j). \quad (26)$$

Further transformations of the first sum in Eq. (26) shows that it represents the coupling of the nuclear to the electronic spin:

$$H^{SO(1)}_{hf}=\mu_B\beta\vec{\sigma}\cdot[\vec{\nabla}\times(\vec{\mu}_n\times\vec{r})A_n(r)]. \quad (27)$$

Inserting the explicit form of the vector potential $A_n(r)$ allows one to split $H^{SO(1)}_{hf}$ into the Fermi contact and spin dipolar hyperfine interaction operators,

$$H_F=2\mu_B\beta\vec{\mu}_n\cdot\vec{\sigma}\frac{1}{r_n^3}\Theta(r_n-r) \quad (28)$$

$$H_{dip}=\mu_B\beta\frac{1}{r^5}[3(\vec{\mu}_n\cdot\vec{r})(\vec{\sigma}\cdot\vec{r})-(\vec{\mu}_n\cdot\vec{\sigma})r^2]\Theta(r-r_n), \tag{29}$$

where the theta functions Θ restrict the operators to the range $r\leqslant r_n$ and $r\geqslant r_n$, respectively. Apart from the factor β, the resulting relativistic operators are obviously very similar to their nonrelativistic counterparts.

Using the gauge property $\vec{\nabla}\cdot\vec{A}_n=0$, the second term $H_{hf}^{SO(2)}$ in Eq. (26) is given by

$$H_{hf}^{SO(2)}=2\mu_B\beta\vec{A}_n\cdot\vec{p}. \tag{30}$$

For the specific nuclear model represented by Eq. (24) one finally has

$$H_{orb}=2\mu_B\beta A_n(r)\vec{\mu}_n\cdot\vec{l}, \tag{31}$$

where we have identified the operator $H_{hf}^{SO(2)}$ in Eq. (30) with the orbital hyperfine operator H_{orb}, that again turns out to be nearly identical to its nonrelativistic counterpart.

Finally, it should be noted that a Gordon decomposition of the hyperfine operator within the framework of Hartree-Fock theory leads to additional terms. In particular a purely relativistic term occurs, that involves a commutator with the nonlocal part of the potential energy entering the Hartree-Fock Hamiltonian.[17]

D. Matrix elements and selection rules

When calculating the matrix elements of the various hyperfine interaction operators, these can be split into a radial and an angular part. In general one has to distinguish between the left- and right-hand solutions $\langle\Phi_\Lambda^L|$ and $|\Phi_{\Lambda'}^R\rangle$, respectively, to the Dirac equation. Fortunately, for the Dirac Hamiltonian given in Eq. (1) the radial wave functions of both sets of solutions are the same for most situations.[25,26] For that reason one has only to distinguish their spin-angular parts, as it is indicated by the superscript $\times$ in Eq. (6). Furthermore, we are interested here in the hyperfine fields of spontaneously magnetized solids. For this type of systems it is in general well justified to assume that the spin and orbital magnetization within an atomic cell are oriented along a common axis, that specifies the local z direction (see above). In that case, it is sufficient in Eqs. (7), (28), (29), and (31) to consider only the z–z part of the scalar products that involve the nuclear magnetic dipole operator $\vec{\mu}_n$.

With this simplification, one gets the conventional expression for the matrix elements connected with the total hyperfine interaction operator H_{hf} given in Eq. (7):[13,20]

$$\langle\Phi_\Lambda^L|H_{hf}|\Phi_{\Lambda'}^R\rangle=-ie\mu_n A_{\Lambda\Lambda'}^{hf}\left[\int_0^{r_n}dr(g_\kappa f_{\kappa'}+f_\kappa g_{\kappa'})\frac{r^3}{r_n^3}+\int_{r_n}^{r_{max}}dr(g_\kappa f_{\kappa'}+f_\kappa g_{\kappa'})\right] \tag{32}$$

with the angular matrix elements

$$A_{\Lambda\Lambda'}^{hf}=i\left[\frac{4\kappa\mu}{4\kappa^2-1}\delta_{\kappa\kappa'}+\sqrt{\frac{1}{4}-\left(\frac{\mu}{\kappa-\kappa'}\right)^2}\,\delta_{\kappa,-\kappa'-1}-\sqrt{\frac{1}{4}-\left(\frac{\mu}{\kappa-\kappa'}\right)^2}\,\delta_{\kappa,-\kappa'+1}\right]\delta_{\mu\mu'}. \tag{33}$$

Here the arguments E and r of the radial wave functions $g_\kappa(r,E)$ and $f_\kappa(r,E)$ as well as their dependency on the magnetic quantum number μ has been suppressed. In addition, the fact that Φ_Λ has in general no unique spin-angular character has been ignored here for the sake of clearness [see Eq. (3)].

In principle, the evaluation of the matrix elements in Eq. (32) implies an integration over the whole space. Because of the short range nature of the magnetic hyperfine interaction [see Eq. (24)], it is well justified to restrict the integration to an atomic cell. Accordingly, r_{max} stands for the muffin tin radius r_{mt} or Wigner-Seitz radius r_{WS} depending on whether a muffin-tin or atomic-sphere-approximation geometry[26] has been adopted for the potential and charge distribution.

As one notes, only mixed combinations of the radial wave functions of the type $g_\kappa f_{\kappa'}$ occur in Eq. (32) because of the structure of the matrices α_i. This is in contrast to the matrix elements of the operators H_F, H_{dip}, and H_{orb}. As a consequence of the Gordon decomposition of the current density, there are only terms connecting two large components or two minor components as, for example, $g_\kappa g_{\kappa'}$.

For the Fermi-contact operator H_F one finds,

$$\langle\Phi_\Lambda^L|H_F|\Phi_{\Lambda'}^R\rangle=2\mu_B\mu_n\left[A_{\Lambda\Lambda'}^F\int_0^{r_n}drg_\kappa g_{\kappa'}\frac{r^2}{r_n^3}-A_{-\Lambda,-\Lambda'}^F\int_0^{r_n}drf_\kappa f_{\kappa'}\frac{r^2}{r_n^3}\right] \tag{34}$$

with the angular matrix elements

$$A_{\Lambda\Lambda'}^F=\left[-\frac{\mu}{\kappa+1/2}\delta_{\kappa\kappa'}-2\sqrt{\frac{1}{4}-\left(\frac{\mu}{\kappa-\kappa'}\right)^2}\,\delta_{\kappa,-\kappa'-1}\right]\delta_{\mu\mu'}. \tag{35}$$

Analogously, the matrix elements of the spin dipolar operator H_{dip} are given by the expression:

$$\langle\Phi_\Lambda^L|H_{dip}|\Phi_{\Lambda'}^R\rangle=\mu_B\mu_n\left[A_{\Lambda\Lambda'}^{dip}\int_{r_n}^{r_{max}}drg_\kappa g_{\kappa'}\frac{1}{r}-A_{-\Lambda,-\Lambda'}^{dip}\int_{r_n}^{r_{max}}drf_\kappa f_{\kappa'}\frac{1}{r}\right] \tag{36}$$

with the corresponding angular matrix elements

$$A^{dip}_{\Lambda\Lambda'}=\left[\frac{4\mu(\kappa+1)}{4\kappa^2-1}\delta_{\kappa\kappa'}-\sqrt{\frac{1}{4}-\left(\frac{\mu}{\kappa-\kappa'}\right)^2}\,\delta_{\kappa,-\kappa'-1}\right.$$
$$\left.-3\sqrt{\frac{1}{4}-\left(\frac{\mu}{\kappa-\kappa'}\right)^2}\,\delta_{\kappa,-\kappa'+1}\right]\delta_{\mu\mu'}. \quad (37)$$

As mentioned above, the relativistic hyperfine operators H_F and H_{dip} are very similar in form to their nonrelativistic counterparts. However, one notes that there might now be contributions to the hyperfine field B_{hf} of non-s electrons via the Fermi-contact operator H_F and of s electrons via the spin dipolar operator H_{dip}. It will be shown below that primarily the $p_{1/2}$ electrons give such unconventional contributions to the hyperfine field via the Fermi-contact operator H_F.

Finally, the matrix elements of the orbital operator H_{orb} are given by the expression:

$$\langle\Phi^L_\Lambda|H_{orb}|\Phi^R_{\Lambda'}\rangle=2\mu_B\mu_n A^{orb}_{\Lambda\Lambda'}\left[\int_0^{r_n}drg_\kappa g_{\kappa'}\frac{r^2}{r_n^3}\right.$$
$$\left.+\int_{r_n}^{r_{max}}drg_\kappa g_{\kappa'}\frac{1}{r}\right]$$
$$-2\mu_B\mu_n A^{orb}_{-\Lambda-\Lambda'}\left[\int_0^{r_n}drf_\kappa f_{\kappa'}\frac{r^2}{r_n^3}\right.$$
$$\left.+\int_{r_n}^{r_{max}}drf_\kappa f_{\kappa'}\frac{1}{r}\right] \quad (38)$$

with the angular matrix elements

$$A^{orb}_{\Lambda\Lambda'}=\left[\frac{\mu(\kappa+1)}{\kappa+1/2}\delta_{\kappa\kappa'}+\sqrt{\frac{1}{4}-\left(\frac{\mu}{\kappa-\kappa'}\right)^2}\,\delta_{\kappa-\kappa'-1}\right]\delta_{\mu\mu'}. \quad (39)$$

As for the operators H_F and H_{dip}, the relativistic orbital hyperfine interaction operator H_{orb} is very similar in form to its nonrelativistic counterpart. However, one has to point out that a finite nucleus has explicitly been assumed in Eq. (31). Accordingly, the corresponding matrix element $\langle\Phi^L_\Lambda|H_{orb}|\Phi^R_{\Lambda'}\rangle$ splits in a natural way into a contribution for $r\leqslant r_n$ and $r\geqslant r_n$ as it can be seen in Eq. (38). As a consequence, there is in principle now an *ordinary* orbital hyperfine field ($r\geqslant r_n$) as well as a *contact* orbital hyperfine field ($r\leqslant r_n$). In practice, however, the contact part will be very small and for that reason this decomposition will not be considered extensively in the following.

The expressions for the various angular matrix elements $A^{hf}_{\Lambda\Lambda'}$, $A^{F}_{\Lambda\Lambda'}$, $A^{dip}_{\Lambda\Lambda'}$, and $A^{orb}_{\Lambda\Lambda'}$ in Eqs. (33), (35), (37), and (39), respectively, are highly symmetric because one may interchange everywhere κ and κ' without changing the result. This property is ensured by the selection rules for κ and κ' and reflects the relationship $A_{\Lambda\Lambda'}=A_{\Lambda'\Lambda}$. Obviously, all angular matrix elements have the common selection rule $\mu=\mu'$, reflecting that the magnetic quantum number μ is a good quantum number even for a spin-polarized solid. For all operators one has a nonvanishing matrix element for $\kappa=\kappa'$ and $\kappa=-\kappa'-1$. These two relations lead to the terms $s_{1/2}$–$s_{1/2}$, $p_{1/2}$–$p_{1/2}$, $p_{3/2}$–$p_{3/2}$, $d_{3/2}$–$d_{3/2}$, ... and $p_{1/2}$–$p_{3/2}$, $d_{3/2}$–$d_{5/2}$, $f_{5/2}$–$f_{7/2}$, ..., respectively, implying the angular momentum selection rule $l=l'$. For the full hyperfine interaction operator H_{hf} one has a third term in Eq. (33) with $\kappa=-\kappa'+1$ leading to $s_{1/2}$–$d_{3/2}$, $p_{3/2}$–$f_{5/2}$, ... and the restriction $l-l'=\pm 2$ for the angular momentum quantum numbers. As one can see from Eq. (37), corresponding terms occur also for the spin dipolar hyperfine operator H_{dip}, while these terms seem to be absent in the case of the Fermi contact and orbital operators H_F and H_{orb}, respectively. However, inspection of Eqs. (35) and (39) shows that nonvanishing matrix elements occur also for the Fermi contact and orbital operators for $\kappa=-\kappa'+1$, because of the coupling mediated via the minor components. For example, for $\kappa=-1$ and $\kappa'=+2$ ($s_{1/2}$–$d_{3/2}$) one has for the minor components the angular matrix element $A_{+1\mu,-2\mu}$, that is nonzero because of the second term in Eq. (35) or (39), respectively. Altogether, one has obviously the same selection rules for all four operators considered above, namely: $\kappa=\kappa'$ and $\kappa=-\kappa'-1$ and $\kappa=-\kappa'+1$, where κ and κ' refer to the spin-angular character of the large components. However, one notes from Eqs. (34) and (38) that the matrix elements for $l-l'=\pm 2$, corresponding to $\kappa=-\kappa'+1$, stem exclusively from the minor components. Only for the spin dipolar operator there is also a contribution via the large components. Because the corresponding radial matrix element involves the product of two radial wave functions with $l-l'=\pm 2$, it is much smaller than those for $l-l'=0$. As a consequence, one can expect that all matrix elements corresponding to the selection rule $\kappa=-\kappa'+1$ are quite small.[13] For this reason these terms will be neglected in the following. An additional justification for this simplification comes from the fact that for the valence states the matrix elements are weighted by the scattering-path operator $\tau_{\Lambda\Lambda'}$. For $l\neq l'$ these quantities are in general quite small compared to the diagonal terms with $l=l'$. This applies in particular for systems with high symmetry.

III. RESULTS AND DISCUSSION

So far only very few fully relativistic calculations for hyperfine fields in magnetically ordered solids can be found in the literature. The pure elements Fe, Co, and Ni have been studied first by Ebert *et al.*[13] using the spin-polarized relativistic Korringa-Kohn-Rostoker (SPR-KKR) formalism sketched in Sec. II. This work was continued by studying diluted[31] and concentrated[14,29] disordered transition metal alloys. In particular the influence of extensions to the plain SDFT Hamiltonian given in Eq. (1) was studied.[29] Apart from these studies one has to mention in addition the work of Shick and Gubanov[32] and Guo and Ebert[3] who used the spin-polarized relativistic linear muffin-tin orbital method of band-structure calculation to investigate among others the pure elements Fe, Co, and Ni as well as transition metal multilayer systems. In the following, results obtained by using the SPR-KKR-CPA method (see Sec. II A) will be presented. In contrast to all previous investigations, a finite size

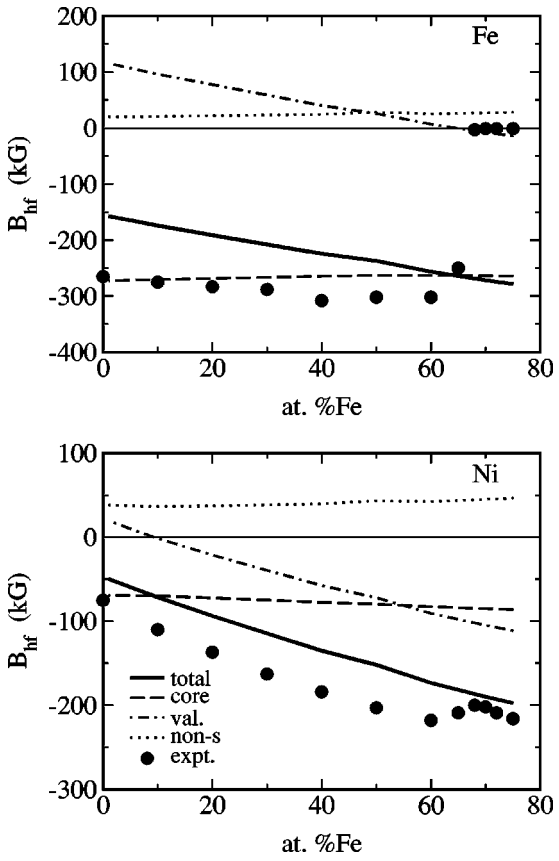

FIG. 1. Hyperfine fields B_{hf} of Fe (top) and Ni (bottom) in the disordered alloy system Fe_xNi_{1-x}. Apart from the total field, the contributions of the core, valence band as well as non-*s* electrons are given separately. Experimental data were taken from Ref. 56.

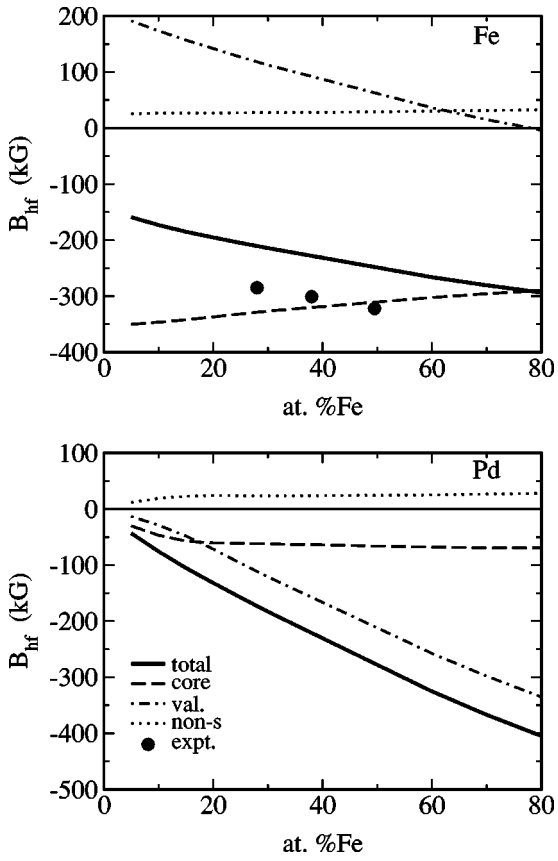

FIG. 2. As for Fig. 1 but for Fe and Pd in Fe_xPd_{1-x}. The experimental data stem from Ref. 56.

for the nucleus has been assumed. The corresponding nuclear radii r_n are for Fe: 8.22×10^{-5} a.u., Co: 8.33×10^{-5} a.u., Ni: 8.44×10^{-5} a.u., Pd: 1.01×10^{-4} a.u., and Pt: 1.23×10^{-4} a.u. These values have been fixed using the empirical relation $r_n=1.128A^{1/3}$ fm (Ref. 33) with A being the mass number for the most abundant isotope.

A. Hyperfine Fields in Fe_xNi_{1-x}, Fe_xPd_{1-x}, and Co_xPt_{1-x}

For the three disordered alloy systems Fe_xNi_{1-x}, Fe_xPd_{1-x}, and Co_xPt_{1-x} the calculated hyperfine fields B_{hf} are given for the various components in Figs. 1–3 as a function of the concentration. The theoretical results are based on the total hyperfine interaction operator given in Eq. (7) and have been split into their core [see Eq. (9)] and valence-band [see Eq. (10)] contributions. To emphasize the relativistic influences, the contributions to B_{hf} due to non-*s* electrons are given separately. In addition, experimental data are shown as far as possible. Comparing the experimental fields with the theoretical results, one finds that the later ones are in general too low. The dependency of the fields on the concentration, on the other hand, is reproduced by the calculations in a rather satisfying way. From the decomposition of the theoretical fields into core and valence-band contributions, B^{core} and B^{val}, respectively, one finds that the concentration dependency is primarily stemming from the valence-band part. In particular one notes that B^{val} changes in several cases its sign, while B^{core} is always negative and varies only moderately with concentration. Because of these properties of B^{core} and B^{val} together with the nearly concentration-independent deviation of the total theoretical from the corresponding experimental fields one may ascribe this deviation to the core contribution. In fact it has been concluded from several previous investigations[10,13,21] that the core-polarization mechanism is not dealt with in a satisfying way within the framework of SDFT. Several attempts to remove these problems by applying self-interaction corrections,[34,35] relativistic corrections to the exchange-correlation potential[35] or gradient corrections to the local-spin-density approximation [Ref. 34] did not improve the situation. Only recently, it could be demonstrated by Akai and Kotani[36] that a construction of the exchange-correlation potential using the optimized-potential method (OPM) leads to a very satisfying agreement with experiment. In particular it turned out, as expected from the previous investigations, that primarily the core hyperfine fields are increased in magnitude, while the remaining contributions are more or less unaffected when applying the OPM scheme.

To get a deeper understanding of the core polarization, the contributions to B^{core} stemming from core *s* and non-*s* electrons are given separately in Figs. 4–6 for Ni, Pd, and Pt, respectively, in the various alloy systems investigated here. As one can clearly see, B^{core} is by far dominated by its *s* contribution. For all $3d$ elements the contribution to B^{core}

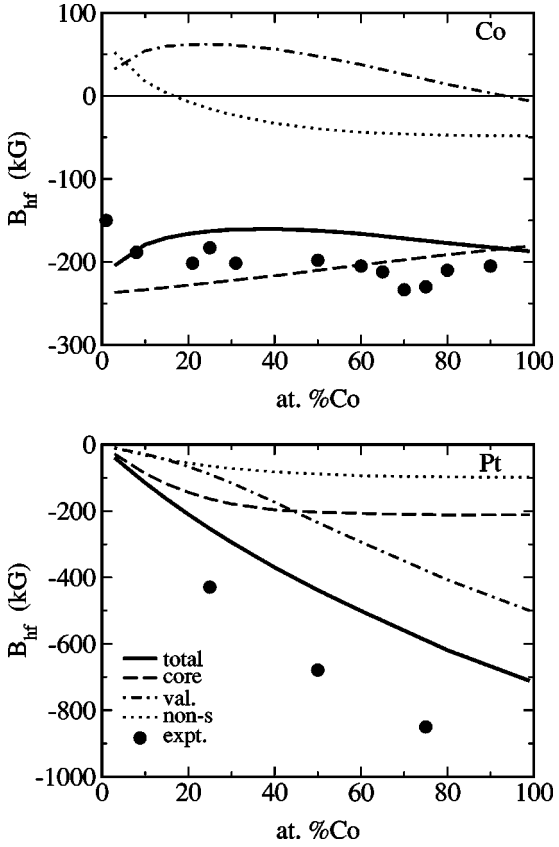

FIG. 3. As for Fig. 1 but for Co and Pt in Co_xPt_{1-x}. The experimental data stem from Ref. 56.

stemming from the $2p$- and $3p$-core shells amounts to about 0.5%. For Pd and Pt, that can be seen to be representative for $4d$- and $5d$-transition metal elements, respectively, the core p-shells contribute 2–3 and around 7%, respectively, while contributions coming from core d and f shells can be ignored. These percentages are more or less independent of the concentration. The rapid increase with atomic number of the non-s contribution to B^{core} points out that these are here of

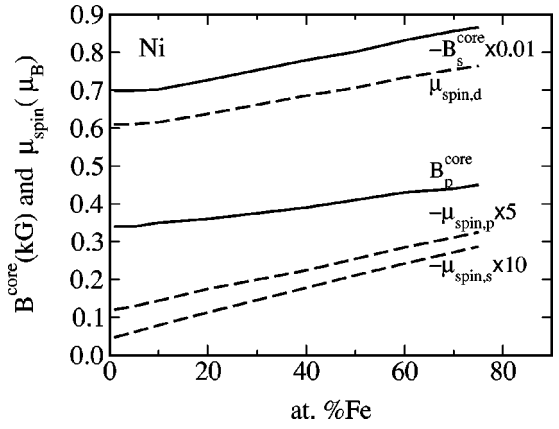

FIG. 4. Angular momentum resolved magnetic moments $\mu_{spin,l}$ and core hyperfine fields B_l^{core} of Ni in Fe_xNi_{1-x}. The contributions of the s and p electrons, B_s^{core} and B_p^{core}, respectively, to the core hyperfine fields are given separately.

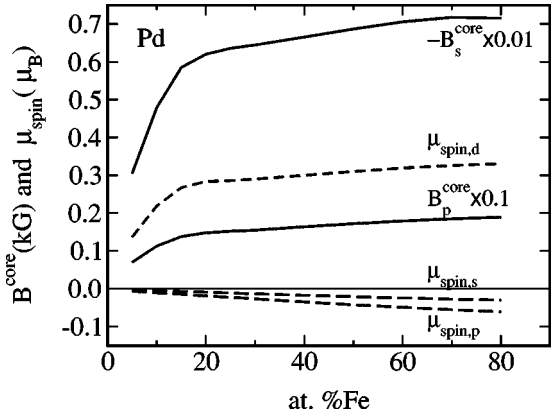

FIG. 5. As for Fig. 4, but for Pd in Fe_xPd_{1-x}.

pure relativistic origin. In fact, within a nonrelativistic or scalar relativistic calculation, such contributions could stem only from the dipolar hyperfine Hamiltonian in the case of noncubic symmetry.

In discussing experimental data for hyperfine fields it is often assumed that there is a simple relationship between the hyperfine field and the various atomic magnetic moments in a multicomponent system.[37–39] One example for such a relation is the expression:[37]

$$B_\alpha = a_\alpha \mu_{spin,\alpha} + b_\alpha \overline{\mu}_{spin}, \tag{40}$$

where α denotes the selected component, $\overline{\mu}_{spin}$ is the average spin moment for the system while a_α and b_α are parameters adjusted to experiment. Previous investigations[37] demonstrated that this expression is in general oversimplified. Nevertheless, one can at least justify the first term as it can be seen in Figs. 4–6. Obviously, the various contributions to B^{core} vary in parallel with the dominating spin magnetic moment $\mu_{spin,d}$ of the d-like valence electrons. As it is demonstrated by the results given in Fig. 7, one finds in particular that the ratios $R_d^{core} = B^{core}/\mu_{spin,d}$ are essentially concentration independent. This applies not only for the s part of B^{core}, but also for its spin-orbit-induced p part.

In the past in general only the ratio $R^{core} = B^{core}/\mu_{spin}$ has been considered within theoretical investigations,[10,16,40–42] where μ_{spin} also includes the contributions

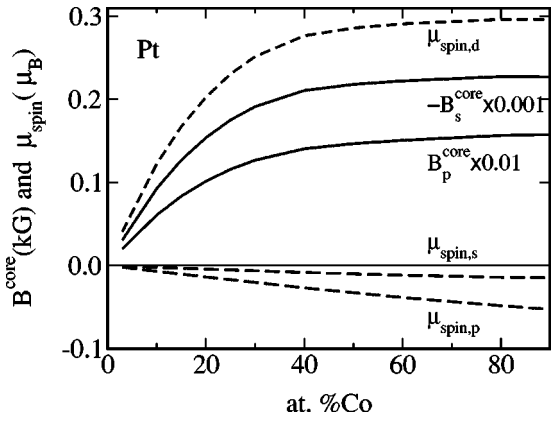

FIG. 6. As for Fig. 4, but for Pt in Co_xPt_{1-x}.

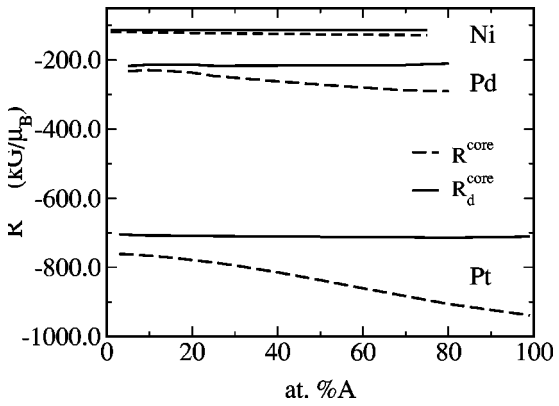

FIG. 7. The ratio $R^{core}=B^{core}/\mu_{spin}$ and $R_d^{core}=B^{core}/\mu_{spin,d}$ for Ni, Pd, and Pt in Fe_xNi_{1-x}, Fe_xPd_{1-x} and Co_xPt_{1-x}, respectively. The concentration refers to the alloy partner A (A=Fe, Co, respectively).

of the *s* and *p* electrons. For Ni, Pd, and Pt some representative values for R^{core} are -124 kG/μ_B, -256 kG/μ_B and -820 kG/μ_B, respectively (these values have been taken for $x_{Ni}=0.8$, $x_{Pd}=0.7$, and $x_{Pt}=0.6$, respectively, from the corresponding dashed curves in Fig. 7). These values are completely in line with previous work. For Ni, for example, Blügel *et al.*[10] found from scalar relativistic calculations $R^{core}=-120$ kG/μ_B, while Ebert[16] obtained -125 kG/μ_B within a fully relativistic calculation. Here one has to note that unlike R_d^{core}, the ratio R^{core} may have a non-negligible concentration dependency. As Fig. 7 shows, this can be ignored for Ni in Fe_xNi_{1-x} but not in the case of Pd and Pt in Fe_xPd_{1-x} and Co_xPt_{1-x}, respectively. The reason for the concentration dependency of R^{core} is obviously the fact that the non-*s* contributions to the spin magnetic moment may have a concentration dependency quite different from that of the *d* electrons. As it can be seen from Fig. 7 this clearly applies for Pd in Fe_xPd_{1-x} and Pt in Co_xPt_{1-x}.

B. Decomposition of the valence hyperfine field

To allow for an analysis of the valence-band hyperfine field B^{val} in analogy to that of the core hyperfine field B^{core} given above, the corresponding angular momentum resolved contributions to B^{val} are given for Fe_xNi_{1-x}, Fe_xPd_{1-x} and Co_xPt_{1-x}, respectively, in Figs. 8–10. One immediately recognizes that for all three alloy systems the magnitude of the valence hyperfine field B^{val} as well as its concentration dependency is essentially given by the *s*-like contributions. Only Co in Co_xPt_{1-x}, for which quite large *d* like contributions occur, makes an exception to this general trend. Quite similar to the situation for the core hyperfine field, one can recognize in Figs. 8 –10 a close relationship of the valence hyperfine field and the spin magnetic moments. Here, however, this one-to-one correspondence is restricted to the *s*-like contributions B_s^{val} and $\mu_{spin,s}$. In addition, one notes that these two quantities are not strictly proportional to one another. This is exemplified by Fe and Co for which B_s^{val} and $\mu_{spin,s}$ change their sign at different concentrations. Nevertheless, one can trace back a major contribution to B_s^{val} to a

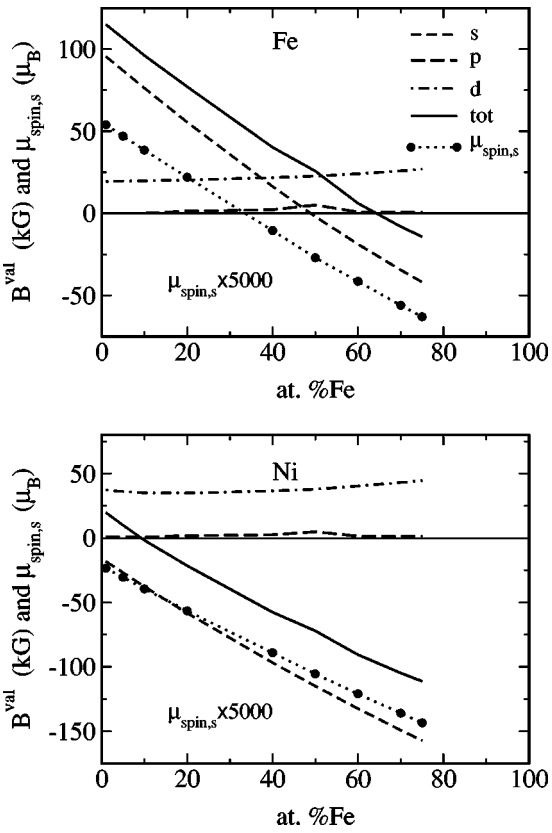

FIG. 8. Valence hyperfine field for Fe (top) and Ni (bottom) in the disordered alloy system Fe_xNi_{1-x}. In addition to the total valence field B^{val} (tot) the *s*, *p*, and *d* contributions are given separately. The line marked with bullets represents the corresponding spin magnetic moment $\mu_{spin,s}$ of the *s* electrons that has been scaled by the given factor.

population difference of the *s*-like minority and majority spin states that is directly reflected by $\mu_{spin,s}$.[43,44] An additional source for B_s^{val} is the polarization of the wave functions due to the surrounding spin magnetization. These sources for B_s^{val} in binary alloys had often been represented by the expression:[39,41,42]

$$B_\alpha = a_\alpha \mu_{spin,\alpha} + b_\alpha \mu_{spin,\alpha} x_\alpha + b_\beta \mu_{spin,\beta}(1-x_\alpha), \tag{41}$$

where β stands for the second alloy partner and a_α, $b_{\alpha(\beta)}$ are fitted to experimental data. Although this ansatz can be justified to some extent on the basis of linear-response theory,[45] one has to emphasize that it leads in general to concentration-dependent fit parameters a_α, $b_{\alpha(\beta)}$.[46] For this reason it is only of limited usefulness in practice.

C. Orbital hyperfine fields

As mentioned already above, the non-*s* contributions to the core hyperfine field B^{core} occur only because of the relativistic formalism used here. This also applies for the contributions to the valence hyperfine field coming from non-*s* electrons. As was shown in Figs. 8–10, these contribute in all cases in an appreciable way to the valence field B^{val}. For Co

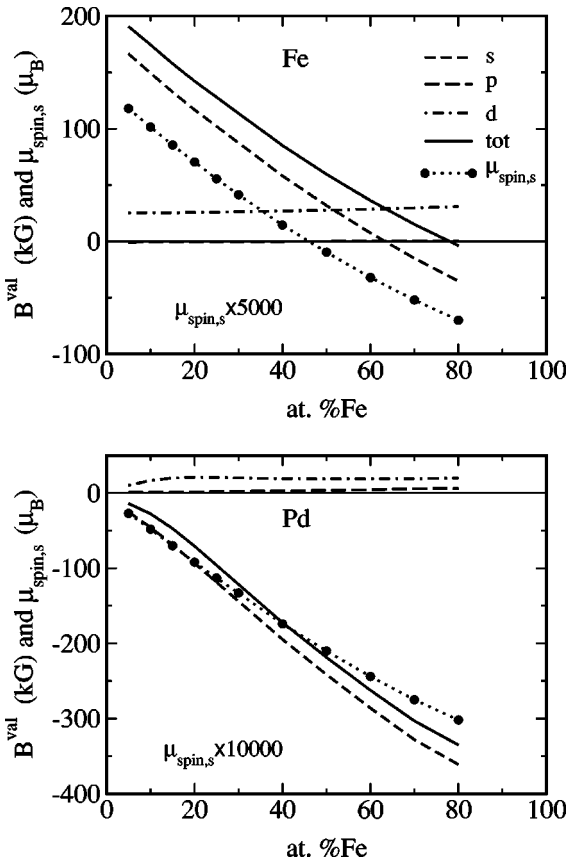

FIG. 9. As for Fig. 8 but for Fe and Pd in Fe_xPd_{1-x}.

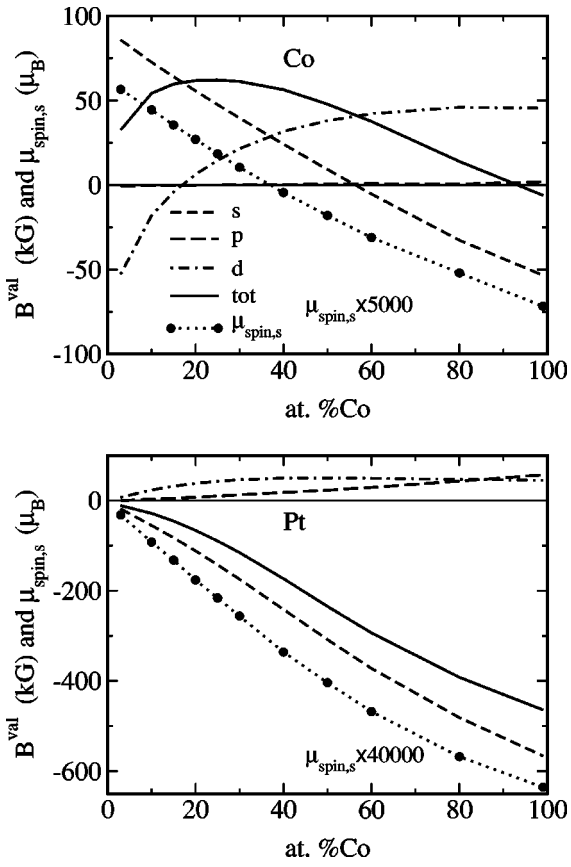

FIG. 10. As for Fig. 8 but for Co and Pt in Co_xPt_{1-x}.

in Co_xPt_{1-x} these contributions even have a remarkable influence on the concentration dependency of the total hyperfine field.

To allow for a more detailed discussion of the hyperfine field contributions B_l^{val} of the non-*s*-valence electrons, these are given in Figs. 11–13 together with the corresponding orbital fields $B_{orb,l}^{val}$. In these figures the fields $B_{orb,p}^{val}$ of the *p* electrons have been omitted for the 3*d* elements, because they are much smaller than those due to the *d* electrons. As it is demonstrated by the results for Pd and Pt, the *p* fields increase quite rapidly with atomic number and for Pt they are in the same order of magnitude as the *d* contributions.

Within a nonrelativistic or scalar relativistic approach the orbital angular momentum is completely quenched in a solid. This quenching of the orbital angular momentum is incomplete if spin-orbit coupling is taken into account and as a consequence there are spin-orbit-induced orbital contributions to the magnetic moment μ_{orb} as well as to the hyperfine field B_{orb}. As mentioned already above, an approximate relationship between these two quantities is supplied by Eq. (12). Accordingly, having calculated $\mu_{orb,l}$, this equation allows to get a reasonable estimate for the orbital hyperfine field $B_{orb,l}^{val}$. For non-*s* electrons the remaining hyperfine fields B_{dip}^{val} due to the dipolar interaction can finally be estimated from,

$$B_{dip}^{val} \approx B_{tot}^{val} - B_{orb}^{val}. \tag{42}$$

In contrast to this approximate approach to decompose the total hyperfine field, the expressions presented in the last section allow in particular a correct and rigorous calculation of the orbital hyperfine field. Corresponding results for the *d*-valence electrons based on Eq. (31) are given in Figs. 11–13 for the various components in the alloy systems Fe_xNi_{1-x}, Fe_xPd_{1-x}, and Co_xPt_{1-x}. Because the hyperfine fields due to *p*-valence electrons increase strongly with atomic number, these are given in addition in the case of Pd and Pt. For comparison Figs. 11–13 also show the corresponding results for the valence electrons with angular momentum *l* obtained on the basis of the relation suggested by Abragam and Pryce. As it can be seen from Fig. 14 for the *d* electrons, the expectation value $\langle r^{-3} \rangle_d$ entering the corresponding Eq. (12) does not vary much with concentration for a given component. As a consequence, the approximate orbital hyperfine field $B_{orb,l}^{val(AP)}$ is essentially proportional to the orbital moment $\mu_{orb,l}$. Although $B_{orb,l}^{val(AP)}$ turns out in most cases to be a reasonable good approximation for the true hyperfine field $B_{orb,l}^{val}$, this does not imply that $B_{orb,l}^{val}$ is strictly proportional to $\mu_{orb,l}$. Co in Co_xPt_{1-x} supplies the most striking example for this, because $B_{orb,l}^{val(AP)}$ and $B_{orb,l}^{val}$ seen as a function of concentration change their sign at different concentrations (see top part of Fig. 13).

Figures 11–13 demonstrate that the reliability of the approximate expression in Eq. (12) varies quite strongly from system to system. For the *d* electrons of Fe in Fe_xNi_{1-x} one finds a remarkable good agreement between $B_{orb,l}^{val(AP)}$ and

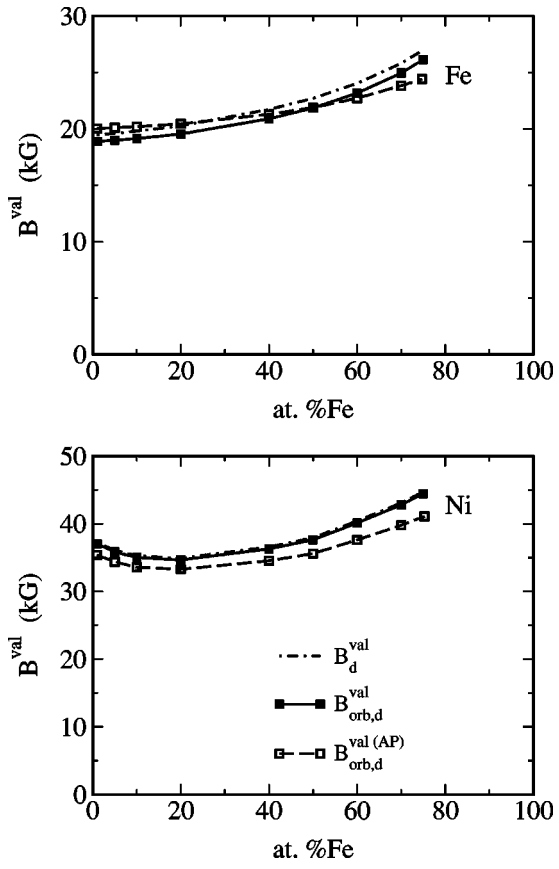

FIG. 11. Orbital and total valence hyperfine fields, $B^{val}_{orb,d}$ and B^{val}_{d}, respectively, for the *d* electrons of Fe (top) and Ni (bottom) in the disordered alloy system Fe_xNi_{1-x}. In addition, the orbital fields $B^{val(AP)}_{orb,d}$ according to the approximate expression due to Abragam and Pryce [Eq. (12)] are given.

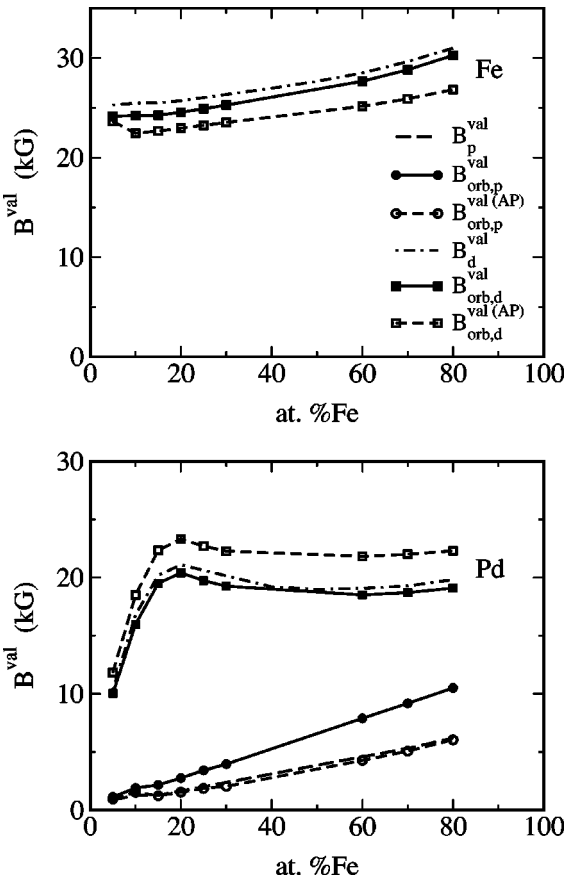

FIG. 12. As for Fig. 11 but for Fe and Pd in Fe_xPd_{1-x}. For Pd the corresponding fields of the *p* electrons are given in addition.

$B^{val}_{orb,l}$. For the other cases investigated here, quite pronounced deviations occur. As mentioned already, the most severe case is Co in Co_xPt_{1-x} when considering the fields of the *d* electrons. But also for the *p* electrons deviations up to 50% may occur as it was found for Pd in Fe_xPd_{1-x}. Due to the very different situations encounterd here, one can expect in spite of these deviations, that Eq. (12) will in many cases supply a reasonable good estimate for the magnitude of the orbital hyperfine field. In particular its concentration dependence should be reproduced quite well, leading to a simple and straightforward connection between this important contribution to the hyperfine field and the orbital magnetic moment.

Comparing the proper orbital field B^{val}_{orb} with the corresponding total hyperfine field of the non-*s*-valence electrons one finds that it gives at least for the *d* electrons the main contribution. This implies that using the term *orbital* for the total field, as it was done in the past,[13,14] is indeed justified to some extent. The difference between the orbital fields B^{val}_{orb} and the corresponding total one B^{val}, that can be quite large, is of course due to the Fermi contact and the dipolar interaction contributions. These will be investigated in more detail in the next section.

D. Correct splitting of the hyperfine fields

In the last section the proper relativistic form for the orbital hyperfine interaction operator given by Eq. (31) has been used to check the quality of the approximate expression given by Abragam and Pryce. In the following, a more detailed analysis of the various parts of the relativistic hyperfine interaction operator in terms of its Fermi contact, dipolar as well as its orbital part will be given.

Because all calculations presented here have been performed assuming a finite-size nucleus, there might in principle be a contribution to the hyperfine field of the *d* electrons via the Fermi-contact term [Eq. (28)]. However, the amplitude of the corresponding wave functions in the nuclear regime is so small that even for Pt the resulting Fermi-contact field is smaller than 10^{-3} kG. As a consequence, the Fermi-contact field can safely be ignored against the other contributions. This implies that the difference between the total and the orbital hyperfine fields of the *d* electrons shown in Figs. 11–13 is due to the dipolar hyperfine interaction [see Eq. (29)]. The corresponding fields are obviously quite small compared with the orbital ones and have in all cases the same sign. Here it is interesting to note that the dipolar fields represent a deviation of the spin magnetization from cubic symmetry that here is only due to the spin-orbit coupling. This means in particular that this field is a direct counterpart to the expectation value of the magnetic dipolar operator $\vec{T}$

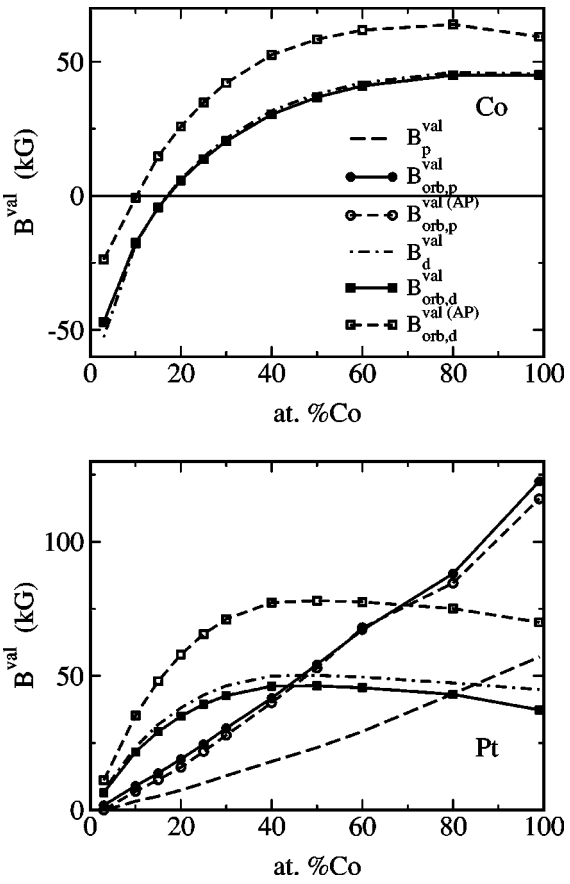

FIG. 13. As for Fig. 11 but for Co and Pt in Co_xPt_{1-x}. For Pt the corresponding fields of the *p* electrons are given in addition.

$=\frac{1}{2}[\vec{\sigma}-3\hat{\vec{r}}(\vec{\sigma}\cdot\hat{\vec{r}})]$. This operator, that—apart from some constants—differs from the dipolar hyperfine interaction operator H_{dip} only by the factor r^{-3}, occurs if one is dealing with the so-called sum rules for the magnetic dichroism in x-ray absorption.[47,48]

When dealing with the *s*- and *p*-like valence electrons the situation gets much more complex than for the *d* electrons.

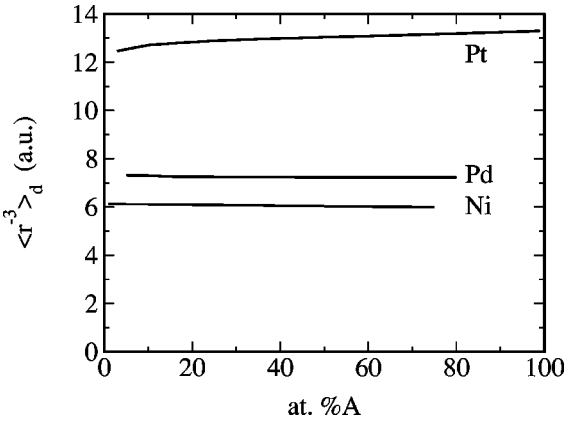

FIG. 14. The expectation value $\langle r^{-3}\rangle_d$ for the *d*-electrons of Ni, Pd, and Pt in Fe_xNi_{1-x}, Fe_xPd_{1-x}, and Co_xPt_{1-x}, respectively. The concentration refers to the alloy partner *A* (*A*=Fe, Co, respectively).

TABLE I. Decomposition of the hyperfine field of the *p* electrons according to the Fermi contact (*F*), dipolar (Dip), and orbital (Orb) hyperfine interaction Hamiltonian. All fields are given in kG.

B_p^{val}	*F*	Dip	Orb	Total
Fe in $Fe_{0.6}Ni_{0.4}$	−0.187	−0.112	0.819	0.520
Ni in $Fe_{0.6}Ni_{0.4}$	−0.307	−0.232	1.577	1.038
Fe in $Fe_{0.6}Pd_{0.4}$	−0.144	0.142	0.169	0.167
Pd in $Fe_{0.6}Pd_{0.4}$	−1.254	−2.460	7.881	4.167
Co in $Co_{0.6}Pt_{0.4}$	−0.149	−0.127	0.782	0.506
Pt in $Co_{0.6}Pt_{0.4}$	−43.484	4.911	67.074	28.501

This is exemplified in Table I that shows the Fermi contact, the dipolar and orbital hyperfine fields of the *p* electrons for the various components of some selected alloys. In line with the fact that these field contributions are of pure relativistic origin, they are rather small compared to the total hyperfine field. Nevertheless, one notes that the Fermi-contact part (first column in Table I) is quite appreciable and in the same order of magnitude as the total field of the *p* electrons (last column in Table I). In addition, one can see that the ratio of the magnitudes of the Fermi contact and total fields increases rapidly with atomic number: 0.29, 0.30, and 1.53, respectively, for the elements Ni, Pd, and Pt listed in Table I. The reason for the occurrence of a Fermi-contact contribution for the *p* electrons, that cannot be understood within a nonrelativistic or scalar relativistic approach, is twofold. On the one hand, as discussed above for the *d* electrons, the wave functions of the *p* electrons penetrate the finite-size nucleus. On the other hand, the relativistic wave function for electrons with $p_{1/2}$ ($\kappa=+1$) character is finite at the nuclear site even for a point nucleus. As a consequence, the total hyperfine field for $p_{1/2}$ electrons is larger than for $p_{3/2}$ electrons, with the difference rapidly increasing with atomic number.[14] From this, one may conclude that the nonvanishing amplitude of the $p_{1/2}$ wave function at the nuclear site ($r=0$) is the main reason for the appreciable Fermi-contact contribution to the hyperfine field of the *p*-valence electrons.

Finally, in Figs. 15–17 the decomposition of the hyperfine fields of the *s*-like valence band electrons is given for the three investigated alloy systems. In all cases one finds a nearly linear dependence on the concentration for the individual contributions. On the basis of a non- or scalar relativistic treatment of the hyperfine interaction, one would expect that the Fermi contact part completely dominates the fields of the *s*-electrons. In contrast to this expectation one finds that the dipolar and orbital part contribute in a substantial way to the total field. This is quite astonishing, because scalar-relativistic calculations, that for cubic systems give a finite hyperfine field only via the Fermi contact Hamiltonian[10] lead in general to results that are very close to the total hyperfine field of the *s*-electrons calculated in a fully relativistic way.[13]

To understand this paradox situation, it is helpful to consider the various angular matrix elements given in Eqs. (35), (37), and (39) for the quantum numbers $\kappa=-1$ and $\mu=\pm 1/2$. From these one finds that the Fermi-contact field stems only from the terms $g_\Lambda g_{\Lambda'}$ and $f_\Lambda f_{\Lambda'}$ [see Eq. (34)] with the same quantum numbers $\Lambda=\Lambda'$, while those with

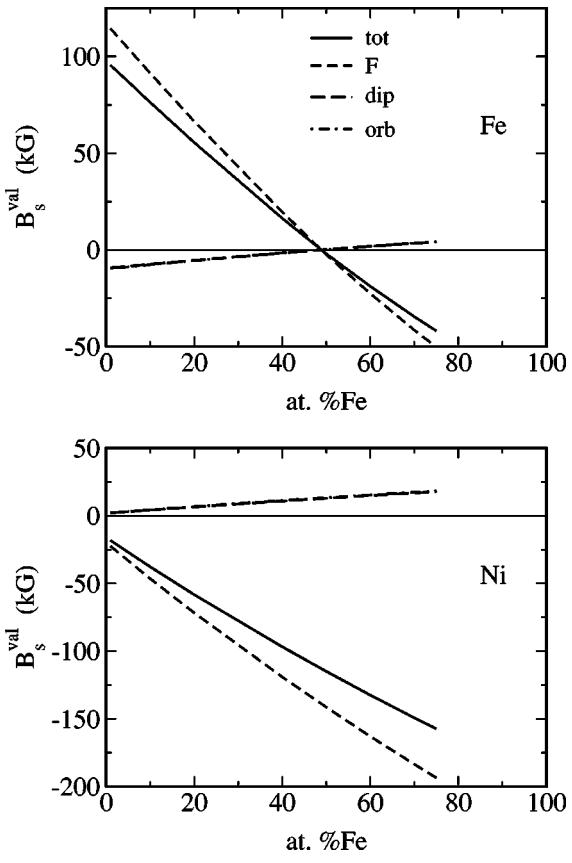

FIG. 15. Fermi contact, dipolar and orbital hyperfine fields for the *s* electrons of Fe (top) and Ni (bottom) in the disordered alloy system Fe_xNi_{1-x}. In addition, the sum of these fields (tot) is given.

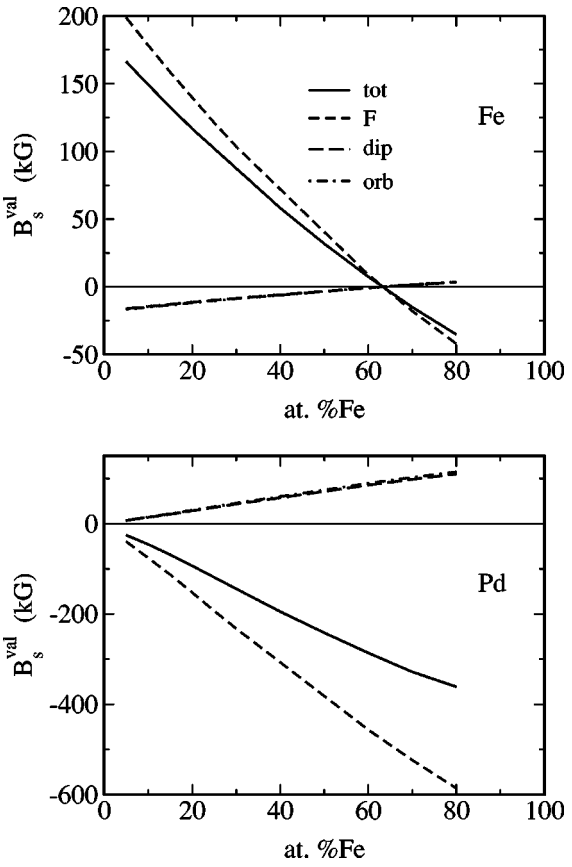

FIG. 16. As for Fig. 15 but for Fe and Pd in Fe_xPd_{1-x}.

$\Lambda \neq \Lambda'$ do not contribute because $A_{\Lambda\Lambda'}=0$. Comparing the contribution of the terms involving the large components g_Λ with that connected with the minor components f_Λ one finds—as to be expected—that the later ones are about two orders of magnitude smaller than the first ones. The dipolar as well as the orbital hyperfine field, on the other hand, stem for *s* states exclusively from terms involving the minor components, because of the selection rules imposed by the angular matrix elements [see Eqs. (37) and (39)]. In addition, it turns out that these are identical, i.e., one has $A^{dip}_{\Lambda\Lambda'}=A^{orb}_{\Lambda\Lambda'}$ for $\kappa=-1$. As a consequence, the resulting dipolar and orbital hyperfine field differ only because the later one includes also contributions from the nuclear region [see Eq. (38)] while the dipolar field is by definition restricted to sources outside the nucleus [see Eq. (36)]. For these reasons the fields $B^{val}_{dip,s}$ and $B^{val}_{orb,s}$ in Figs. 15–17 are nearly identical for the $3d$ elements and also for Pd. Only for Pt in Co_xPt_{1-x} remarkable differences are found (lower part of Fig. 17). Finally, one has to note that from the Eqs. (34), (35), (38), and (39) one deduces the simple relationship $B^{(in)}_{orb,s}=-2B^{(f)}_{F,s}$, where the superscript *(in)* indicates that only the region $r \leqslant r_n$ is considered for the integration in Eq. (38) and (f) indicates the contribution of the minor components to the Fermi-contact field.[17]

If one considers the limit of a vanishing nuclear radius for the matrix elements of the total hyperfine operator [Eq. (7)] one is led to a finite result because the product of a large and a minor component is involved [Eq. (34)]. The expression for the matrix elements of the Fermi-contact Hamiltonian, on the other hand, diverges for a vanishing nuclear radius in the case of $s_{1/2}$ and $p_{1/2}$ states.[17] Because the sum of the individual Fermi contact, dipolar and orbital contributions converges, one has to conclude that the later two terms also diverge as it can be seen directly from the explicit expressions given in Eqs. (36) and (38). This implies that in the limit of a point nucleus the individual contributions will loose their original meaning. Furthermore, one notes that for $s_{1/2}$ and also for $p_{1/2}$ electrons the magnitude of the individual terms depend very sensitively on the size of the nucleus. For that reason a direct comparison of scalar-relativistic hyperfine fields is only meaningful if these are compared with the total relativistic hyperfine field. Here it should be noted that the conventional nonrelativistic description of the hyperfine interaction is recovered from the relativistic operators given in Eqs. (28), (29), and (31) by first considering the limit $c \to \infty$ for the speed of light c.[17] This leads to the nonrelativistic wave functions and hyperfine interaction operator. Finally, the limit $r_n \to 0$ has to be taken.

E. Interpretation of the hyperfine field contributions and their dependence on the nuclear radius r_n

To investigate the relationship of the total hyperfine field and the chosen nuclear model we consider in the following the case of an Au-impurity dissolved substitutionally in bcc

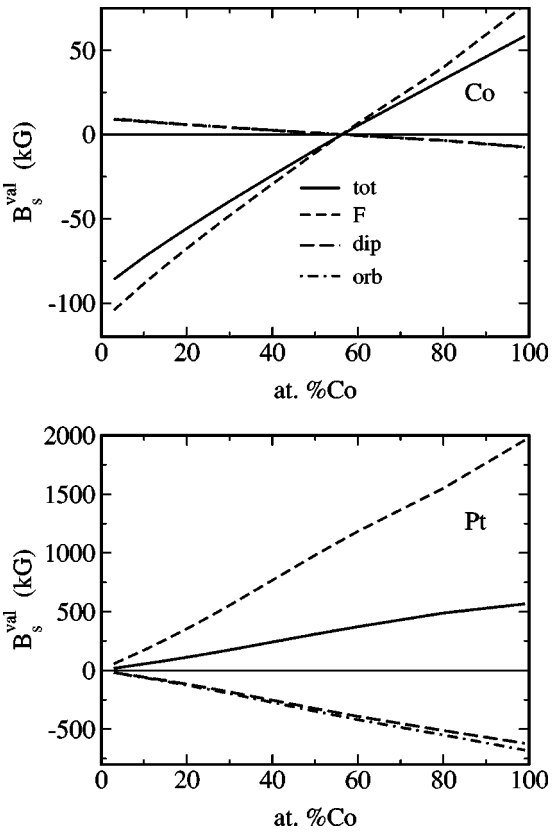

FIG. 17. As for Fig. 15 but for Co and Pt in Co_xPt_{1-x}.

Fe. The corresponding calculations have been performed in just the same way as for, e.g., the alloy system Co_xPt_{1-x} in the limit $x \to 1$. In particular the potential distortion of the host in the vicinity of the impurity as well as the relaxation of the lattice has been ignored.

The Fermi contact, dipolar, orbital, and total hyperfine fields of Au obtained this way are given in Table II in an angular momentum resolved way. For these calculations the nuclear radius has been set to $r_n = 1.2396 \times 10^{-4}$ a.u. according to the mass number $A = 197$. As one can see from Table II, the major contributions to the hyperfine field stem from the *s* electrons. According to the analysis given above, these stem primarily from the region outside the nucleus $B_s^{(out)} = B_{dip,s} + B_{orb,s}^{(out)} = 2B_{dip,s} = 2031.8$ kG. With this the total contact field, i.e., Fermi contact plus orbital part, is given as: $B_{contact,s} = B_{F,s} + B_{orb,s}^{(in)} = B_{F,s} + B_{orb,s} - B_{dip,s} = -2967.2$ kG, where the orbital part $B_{orb,s}^{(in)}$ contributes only 76.4 kG. For *p* states a corresponding decomposition is less straightforward because the spin-orbit coupling splits these into states with $p_{1/2}$ and $p_{3/2}$ character, respectively. However, an analysis of the numerical results for the core *p* states reveals that the Fermi-contact field is primarily due to $p_{1/2}$ states. In addition, one can ascribe this contribution exclusively to the corresponding minor component that has the spin-orbit character $\kappa = -1$. This once more points out that it is of pure relativistic origin.

TABLE II. Angular resolved contributions of the core and valence hyperfine fields (in kG) for Au in Fe. These values have been obtained using a finite size nucleus with $r_n = 1.2396 \times 10^{-4}$ a.u.

Core	*F*	Dip	Orb	Tot
s	−713.2	238.1	256.0	−219.2
p	−16.3	3.4	29.7	16.8
d	0.0	−0.0	−0.4	−0.4
f	0.0	−0.0	−0.1	−0.1
Tot	−729.5	241.4	285.2	−202.9
Valence				
s	−2330.3	777.2	835.7	−717.3
p	−113.4	12.6	172.3	71.5
d	0.0	3.2	67.6	70.8
Tot	−2443.7	793.0	1075.6	−575.1

While the core hyperfine field of the *d*- and *f*-electron shells are completely negligible, there is a rather large field due to the *d*-like valence electrons. This in turn is dominated by its orbital part, that is connected with the spin-orbit-induced orbital polarization of the *d* electrons (see above).

For elements that have several isotopes with a finite magnetic moment, a determination of the hyperfine fields, e.g., via NMR leads in general to different fields for the various isotopes. This so-called hyperfine anomaly has been used in the past to derive noncontact hyperfine fields from experiment.[49–51] For this, one assumes that the fields of the various isotopes differ only with respect to the contributions stemming from the nuclear region, while the remaining contributions are independent of the isotope or nuclear properties, respectively.[52] Usually the noncontact fields deduced from investigations based on the hyperfine anomaly are called *orbital* fields. For Au in Fe Kawakami *et al.*,[51] obtained the value 161 ± 26 kG. Unfortunately, a direct comparison of this field with the orbital fields given above is however not meaningful because these are based on different considerations.

To allow for a direct comparison it is sensible to investigate the dependence of the hyperfine field on the nuclear radius r_n to find out which of its parts is independent of the nuclear size. For this purpose additional calculations have been done with the nuclear radius decreased and increased by 10%. The resulting relative changes with respect to the first set of calculations (see Table II) are summarized in Table III. As it was to be expected, the various contributions of the *s* electrons changed quite strongly with the nuclear radius, although the corresponding total field shows only a relatively small increase with r_n. This behavior has its origin in the dependency of the various radial integrals on the nuclear radius, as it was discussed above. The contact field increases in magnitude roughly to the same extent as the sum of the orbital and dipolar fields. Because of their different sign these changes nearly compensate each other. The same behavior is found for the various contributions to the core and valence hyperfine field. It is remarkable that the most pronounced changes are found for the dipolar contributions

TABLE III. Changes in % of the various hyperfine field contributions for Au in Fe for calculations using the nuclear radii $r_1 = 1.1396 \times 10^{-4}$ a.u. and $r_2 = 1.3596 \times 10^{-4}$ a.u. with respect to the values given in Table II obtained for $r_n = 1.2396 \times 10^{-4}$ ($r_1/r_n = 0.919$; $r_2/r_n = 1.096$).

Core	F		Dip		Orb		Tot	
	r_1	r_2	r_1	r_2	r_1	r_2	r_1	r_2
s	3.36	−3.62	4.65	−4.94	4.56	−4.85	0.64	−0.74
p	3.19	−3.39	7.33	−7.75	1.03	−1.11	0.20	−0.22
d	0.00	0.00	0.00	0.00	0.00	0.00	0.00	0.00
f	0.00	0.00	0.00	0.00	0.00	0.00	0.00	0.00
Valence								
s	3.35	−3.57	4.62	−4.90	4.53	−4.81	0.61	−0.70
p	3.16	−3.36	13.35	−14.13	1.23	−0.98	0.31	−0.36
d	0.00	0.00	0.03	0.00	0.00	−0.01	0.00	0.00

of the p electrons. Obviously, these depend quite strongly on the electronic properties in the vicinity of the nuclear radius. For the hyperfine fields of the d and f electrons on the other hand, the changes with the nuclear radius can be neglected.

From these findings one has first of all to point out that the use of the term *orbital* hyperfine field for the theoretical field is consistent because of the occurrence of the orbital angular momentum operator in Eq. (38). However, a direct comparison with the noncontact hyperfine fields deduced from experiment via the hyperfine anomaly is not allowed. To look for a relationship with the experimental noncontact hyperfine fields it would be sensible to consider only the orbital p as well as the d and f fields given in Table III, because of their very weak dependence on the nuclear radius. This way one gets for Au in Fe the value 272 kG, that lies about 100 kG above its experimental counterpart. An alternative to this procedure is to sum all field contributions of the non-s electrons.[16] This leads to a noncontact field of 159 kG that is in very good agreement with the experimental value. However, the same procedure leads for Ir in Fe to a theoretical noncontact field of −26.6 kG. Experimental values, based on a number of auxiliary assumptions, are 300 ± 200 kG [Ref. 53] and 155 ± 90 kG.[54] These values are reasonably well reproduced if one takes within the theoretical considerations for the p electrons only the orbital part, leading to +73.5 kG. In conclusion, one has to say that the calculations presented here were not able to explain the available experimental data for the noncontact fields in a consistent and satisfying way. One reason for this could be that some of the assumptions, on which the analysis of the experimental data relies, are not fully justified. Another possible source for the discrepancy is the chosen nuclear model, that is quite unrealistic concerning its assumption on the distribution of the nuclear magnetization. For these reasons, to deal with the hyperfine anomaly in a more proper way, it seems to be desirable to adopt a more realistic nuclear model. In particular it should include the Bohr-Weisskopf correction,[55] that accounts for the spatial distribution of the magnetic dipole moment within the nuclear regime and its influence on the hyperfine interaction. Setting up the model specific for a given isotope, one can compare the resulting hyperfine field directly with experiment and it does not have to rely on an additional analysis of the experimental data.

IV. SUMMARY

A scheme developed by Pyper within the framework of Hartree-Fock theory has been modified to allow a rigorous decomposition of the hyperfine fields calculated in a fully relativistic way on the basis of spin-density-functional theory. This decomposition into a Fermi contact, dipolar, and orbital part requires the adoption of a finite nuclear model. Compared to a nonrelativistic or scalar relativistic approach one arrives at the striking consequence that one may have a Fermi-contact contribution also from non-s electrons and dipolar as well as orbital contributions stemming from s electrons. Corresponding calculations have been performed for the disordered substitutional ferromagnetic alloy systems fcc Fe_xNi_{1-x}, fcc Fe_xPd_{1-x}, and fcc Co_xPt_{1-x} making use of the spin-polarized relativistic version of the KKR-CPA method of band-structure calculation. These calculations revealed pronounced influences of relativistic effects on the hyperfine fields. In particular, appreciable contributions from non-s electrons were obtained that cannot be understood within a nonrelativistic or scalar relativistic theory. An estimate of the orbital hyperfine field on the basis of an expression suggested by Abragam and Pryce has shown that these non-s fields are primarily of orbital origin. This could be confirmed by making use of the rigorous decomposition of the total fields into their Fermi contact, dipolar and orbital parts. For d electrons it turned out that, as expected earlier, the orbital part strongly dominates. For p electrons, on the other hand, one finds indeed appreciable dipolar contributions to the total field. Finally, for the s electrons there are rather pronounced dipolar and orbital fields. These are exclusively connected with the minor component of the four-component wave function and increase rapidly with atomic number. A calculation of the various field contributions for different nuclear radii revealed in the case of Au in Fe a rather sensitive dependency. However, a satisfying interpretation of the results of experimental hyperfine anomaly investigations seems to be somewhat problematic. Because of this, it is suggested to use a more realistic nuclear model for this purpose, that allows a more rigorous investigation of the isotope effects.

ACKNOWLEDGMENTS

This work was funded by the DFG (Deutsche Forschungsgemeinschaft) within the program *Theorie relativistischer Effekte in der Chemie und Physik schwerer Elemente* and benefited from collaborations within the European TMR-network on *Ab-initio Calculations of Magnetic Properties of Surfaces, Interfaces, and Multilayers*.

[1] E. Fermi, Z. Phys. **60**, 320 (1930).
[2] J. D. Jackson, *Classical Electrodynamics* (Wiley, New York, 1962).
[3] G. Y. Guo and H. Ebert, Phys. Rev. B **53**, 2492 (1996).
[4] C. G. Darwin, Proc. R. Soc. London, Ser. A **118**, 654 (1928).
[5] W. Gordon, Z. Phys. **48**, 11 (1928).
[6] G. Breit, Phys. Rev. **35**, 1447 (1930).
[7] P. Pyykkö, E. Pajanne, and M. Inokuti, Int. J. Quantum Chem. **VII**, 785 (1973).
[8] T. Asada and K. Terakura, J. Phys. F: Met. Phys. **12**, 1387 (1982).
[9] C. L. Fu and A. J. Freeman, J. Magn. Magn. Mater. **69**, L1 (1987).
[10] S. Blügel, H. Akai, R. Zeller, and P. H. Dederichs, Phys. Rev. B **35**, 3271 (1987).
[11] G. Breit, Phys. Rev. **38**, 463 (1931).
[12] L. Tterlikkis, S. D. Mahanti, and T. P. Das, Phys. Rev. **178**, 630 (1969).
[13] H. Ebert, P. Strange, and B. L. Gyorffy, J. Phys. F: Met. Phys. **18**, L135 (1988).
[14] H. Ebert and H. Akai, Hyperfine Interact. **78**, 361 (1993).
[15] A. Abragam and M. H. L. Pryce, Proc. R. Soc. London, Ser. A **205**, 135 (1951).
[16] H. Ebert, Habilitation thesis, University of München, 1990.
[17] N. C. Pyper, Mol. Phys. **64**, 933 (1988).
[18] A. H. MacDonald and S. H. Vosko, J. Phys. C **12**, 2977 (1979).
[19] A. H. MacDonald, J. Phys. C **16**, 3869 (1983).
[20] M. E. Rose, *Relativistic Electron Theory* (Wiley, New York, 1961).
[21] H. Ebert, J. Phys.: Condens. Matter **1**, 9111 (1989).
[22] P. Weinberger, *Electron Scattering Theory for Ordered and Disordered Matter* (Oxford University Press, Oxford, 1990).
[23] H. Ebert, in *Electronic Structure and Physical Properties of Solids*, edited by H. Dreyssé, Lecture Notes in Physics, Vol. 535 (Springer, Berlin, 2000), p. 191.
[24] G. Hörmandinger and P. Weinberger, J. Phys.: Condens. Matter **4**, 2185 (1992).
[25] E. Tamura, Phys. Rev. B **45**, 3271 (1992).
[26] T. Huhne, C. Zecha, H. Ebert, P. H. Dederichs, and R. Zeller, Phys. Rev. B **58**, 10 236 (1998).
[27] L. Nordström and D. J. Singh, Phys. Rev. Lett. **76**, 4420 (1996).
[28] H. Ebert, M. Battocletti, and E. K. U. Gross, Europhys. Lett. **40**, 545 (1997).
[29] H. Ebert and M. Battocletti, Solid State Commun. **98**, 785 (1996).
[30] M. S. S. Brooks, Physica B & C **130**, 6 (1985).
[31] H. Ebert, R. Zeller, B. Drittler, and P. H. Dederichs, J. Appl. Phys. **67**, 4576 (1990).
[32] A. B. Shick and V. A. Gubanov, Phys. Rev. B **49**, 12 860 (1994).
[33] T. Mayer-Kuckuk, *Kernphysik* (Teubner, Stuttgart, 1984).
[34] M. Battocletti, H. Ebert, and H. Akai, Phys. Rev. B **53**, 9776 (1996).
[35] L. Severin, M. Richter, and L. Steinbeck, Phys. Rev. B **55**, 9211 (1997).
[36] H. Akai and T. Kotani, Hyperfine Interact. **120–121**, 3 (1999).
[37] C. E. Johnson, M. S. Ridout, T. E. Cranshaw, and P. E. Madsen, Phys. Rev. Lett. **6**, 450 (1961).
[38] U. Erich, Z. Phys. **227**, 25 (1969).
[39] N. J. Stone, in *Low-temperature nuclear orientation*, edited by N. L. Stone and H. Postma (North-Holland, Amsterdam, 1986), p. 351.
[40] S. Hüfner, Phys. Rev. B **1**, 2348 (1970).
[41] K. Takanashi, H. Yasuoka, K. Kawaguchi, N. Hosoito, and T. Shinjo, J. Phys. Soc. Jpn. **51**, 3743 (1982).
[42] Y. Muraoka, M. Shiga, H. Yasuoka, and Y. Nakamura, J. Phys. Soc. Jpn. **40**, 414 (1976).
[43] H. Ebert, H. Winter, D. D. Johnson, and F. J. Pinski, Hyperfine Interact. **51**, 925 (1989).
[44] H. Ebert, H. Winter D. D. Johnson, and F. J. Pinski, J. Phys.: Condens. Matter **2**, 443 (1990).
[45] H. Ebert (unpublished).
[46] H. H. Hamdeh, B. Fultz, and D. H. Pearson, Phys. Rev. B **39**, 11 233 (1989).
[47] B. T. Thole, P. Carra, F. Sette, and G. van der Laan, Phys. Rev. Lett. **68**, 1943 (1992).
[48] P. Carra, B. T. Thole, M. Altarelli, and X. Wang, Phys. Rev. Lett. **70**, 694 (1993).
[49] F. E. Wagner, Hyperfine Interact. **13**, 149 (1983).
[50] E. Hagn and E. Zech, Phys. Rev. B **29**, 1148 (1984).
[51] M. Kawakami, H. Enokiya, and T. Okamoto, J. Phys. F: Met. Phys. **15**, 1613 (1985).
[52] R. Fox and N. J. Stone, Phys. Rev. Lett. **29**, 341 (1969).
[53] G. J. Perlow, W. Henning, D. Olson, and G. Goodman, Phys. Rev. Lett. **23**, 680 (1969).
[54] F. E. Wagner and W. Potzel, in *Hyperfine Interactions in Excited Nuclei*, edited by G. Goldring and R. Lalish (Gordon and Breach, New York, 1971), p. 681.
[55] A. Bohr and V. F. Weisskopf, Phys. Rev. **77**, 94 (1950).
[56] M. B. Stearns, in *Magnetic Properties of 3d, 4d and 5d Elements, Alloys and Compounds*, edited by K.-H. Hellwege and O. Madelung, Landolt-Börnstein, Group III, Vol. 19, Pt. a (Springer, Berlin, 1987).